

Epidermal Snail expression drives skin cancer initiation and progression through enhanced cytoprotection, epidermal stem/progenitor cell expansion and enhanced metastatic potential

B De Craene^{1,2}, G Denecker^{1,2}, P Vermassen^{1,2}, J Taminiau^{1,2}, C Mauch³, A Derore², J Jonkers⁴, E Fuchs⁵ and G Berrx^{*,1,2}

Expression of the EMT-inducing transcription factor Snail is enhanced in different human cancers. To investigate the *in vivo* role of Snail during progression of epithelial cancer, we used a mouse model with skin-specific overexpression of Snail. Snail transgenic mice spontaneously developed distinct histological subtypes of skin cancer, such as basal cell carcinoma, squamous cell carcinoma and sebaceous gland carcinoma. Development of sebaceous gland carcinomas strongly correlated with the direct and complete repression of Blimp-1, a central regulator of sebocyte homeostasis. Snail expression in keratinocyte stem cells significantly promotes their proliferation associated with an activated FoxM1 gene expression signature, resulting in a larger pool of Mts24-marked progenitor cells. Furthermore, primary keratinocytes expressing Snail showed increased survival and strong resistance to genotoxic stress. Snail expression in a skin-specific p53-null background resulted in accelerated formation of spontaneous tumours and enhanced metastasis. Our data demonstrate that *in vivo* expression of Snail results in *de novo* epithelial carcinogenesis by allowing enhanced survival, expansion of the cancer stem cell pool with accumulated DNA damage, a block in terminal differentiation and increased proliferation rates of tumour-initiating cells.

Cell Death and Differentiation (2014) 21, 310–320; doi:10.1038/cdd.2013.148; published online 25 October 2013

During tumour progression, epithelial cancer cells can undergo a dedifferentiation process and transition from a collective invasion front to disseminated migratory detachment of cells capable of spreading to distinct sites throughout the body.¹ Epithelial to mesenchymal transition (EMT) is an important step in this transition that is characterised by loss of adherence markers such as E-cadherin and increased migratory potential. Once the tumour has achieved the dedifferentiated state of single-cell dissemination, metastatic spread is increased and prognosis is exacerbated.² The transcription factor Snail (Snail homolog 1, Snai1) is a direct transcriptional repressor of E-cadherin^{3,4} and its overexpression *in vitro* and subsequent microarray analysis has clearly demonstrated its cellular reprogramming capacity and has underscored the potential role of Snail as a master regulator of EMT.^{5,6}

Evidence correlating Snail to invasion has been found in many human and non-human cell lines. Although there is a large amount of *in vitro* data describing the role of Snail in numerous signalling cascades, one of the most important remaining challenges in the EMT field is to unravel its *in vivo* role in carcinogenesis and metastasis. In this respect, Snail expression has been detected in recurrent breast cancer cells with enhanced *HER2/neu* expression.⁷ When Snail expression

is blocked in human breast cancer cell lines,⁸ the cells undergo a partial MET (mesenchymal to epithelial transition), and their tumourigenic behaviour in xenograft assays is reduced. The advent of well-characterised monoclonal antibodies specifically recognising Snail has been instrumental in demonstrating its expression in a wide range of epithelial tumours and in activated stromal cells surrounding the tumour.²

Snail expression studies related to skin cancer are modest at best. Indirect evidence for a potentially important contribution of Snail has been provided by only a few studies on mice and has largely been correlative in nature. Demethylation of the Snail promoter has been observed in a multistage skin carcinogenesis model used to study epigenetic alterations coinciding with the transition from epithelial to mesenchymal morphology.⁹ In other transgenic mouse models, Snai1 expression was detected downstream of Gli-1¹⁰ and TGF- β signalling.¹¹

To gain further insight into the specific *in vivo* role of Snail during skin cancer progression, we used a combined immunohistochemical analysis of a variety of human skin cancers along with a mouse model with skin-specific expression of an HA-tagged Snail protein.¹² Here we report for the first time that Snail transgenic mice develop spontaneous

¹Unit of Molecular and Cellular Oncology, Inflammation Research Center (IRC), VIB-Ghent University, Ghent, Belgium; ²Department of Biomedical Molecular Biology, Ghent University, Ghent, Belgium; ³Department of Dermatology, University of Cologne, Cologne, Germany; ⁴Division of Molecular Biology, The Netherlands Cancer Institute, Amsterdam, The Netherlands and ⁵Laboratory of Mammalian Cell Biology and Development, The Rockefeller University, New York, NY, USA

*Corresponding author: G Berrx, Unit of Molecular and Cellular Oncology, Inflammation Research Center (IRC), VIB-Ghent University, Technologiepark 927, Ghent (Zwijnaarde) B-9052, Belgium. Tel: +32 9 331 3660; Fax: +32 9 331 36 09; E-mail: Geert.Berrx@dmbr.VIB-UGent.be

Keywords: skin cancer; EMT; Snail; stem cells

Abbreviations: BCC, basal cell carcinoma; DMBA, 2,4-dimethoxybenzaldehyde; EMT, epithelial to mesenchymal transition; H&E, hematoxylin and eosin; MET, mesenchymal to epithelial transition; SCC, squamous cell carcinoma; TPA, 12-*O*-tetradecanoylphorbol-13-acetate; WT, wild type

Received 4.4.13; revised 29.8.13; accepted 13.9.13; Edited by G Melino; published online 25.10.2013

tumours: our results indicate that enhanced Snail expression contributes to the stabilisation, expansion and survival of skin stem cells *in vivo*, which can result in both skin tumour initiation and malignant progression for a variety of epithelial-derived tumour types.

Results

Snail is expressed in different types of human skin cancer. Analysis of Snail expression has been carried out in different types of primary human cancers, including breast, colon and stomach cancer.¹³ To increase our knowledge on expression of this transcription factor in skin cancer, we stained a panel of basal cell carcinoma (BCC) samples with a well-characterised monoclonal Snail antibody.¹⁴ In all, 16.6% of these samples were Snail-positive (Table 1). However,

Table 1 Detection of Snail expression in a panel of human skin tumours

Pathological classification	Positive samples/total
Basal cell carcinoma	5/30
Poroma/porocarcinoma	4/6
Sebaceous gland carcinoma	1/4
Trichoblastoma	1/2

The pathological classification of the different skin tumours stained in this study and the number of samples that are immunoreactive with Snail

Snail expression was evident only at invasive fronts, where cells seem to undergo EMT (Supplementary Figure S1). Furthermore, we stained an additional group of 21 pathologically different skin tumours (Table 1), 28.6% showed enhanced Snail immunoreactivity. Although we stained only a few poroma and porocarcinoma samples, many of these samples were Snail-positive. As reported previously,¹⁴ some tumours expressed Snail in the activated stroma close to the invasive regions and occasionally in endothelial cells. These results show that a variety of human skin cancers have aberrantly activated and stabilised Snail expression in the most histologically invasive regions of these tumour samples.

Snail expression in skin induces spontaneous tumour formation. The frequent expression of Snail in a wide variety of human skin tumour samples prompted us to investigate whether Snail expression is sufficient to drive tumour progression in an *in vivo* mouse model. Sustained Snail expression in the basal layer of the skin leads to epidermal hyperproliferation resulting in increased epidermal thickness in *K14-Snail* mice.¹² Quantification of Ki-67-positive cells in Snail-positive skin further supports this enhanced proliferation rate (Figures 1a and b).

Surprisingly, *K14-Snail* mice started to develop spontaneous skin tumours at the age of 5 months, with a median latency of 282 days (Supplementary Table S1). Histological analysis of these tumours revealed three major epithelial

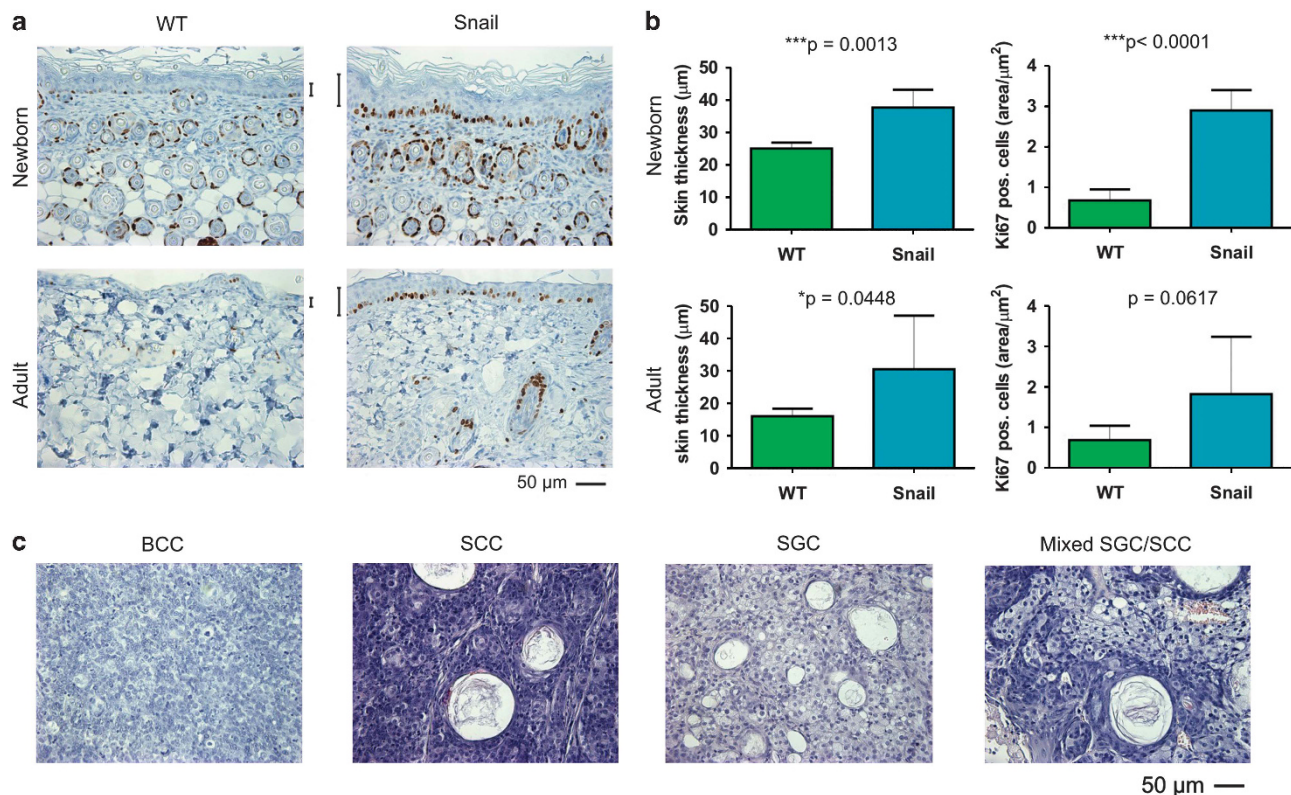


Figure 1 Spontaneous tumour formation in *K14-Snail* mice. (a) Histological analysis of Ki67 expression in *K14-Snail* and WT control mice at the ages of 6 days and 4 months. Bars indicate epidermal thickness. (b) Measurement of skin thickness and Ki67-positive cell counts (right panel) in three WT and three *K14-Snail* mice (newborn) and five WT and four *K14-Snail* mice (adult). (c) Histological analysis of sections stained with H&E reveals distinct tumour types, such as sebaceous gland carcinoma (SGC) (40%), BCC (6.67%) and SCC (13.33%). Mixed tumours were also identified (40%)

tumour types, including BCC, squamous cell carcinoma (SCC) and sebaceous gland carcinoma (Supplementary Table SII). Sebaceous gland carcinoma in *K14-Snail* mice was often mixed with SCC implying an early progenitor population that becomes transformed but still retains some differentiation characteristics (Figure 1c).

Snail expression represses Blimp-1 and results in sebocyte amplification. One of the most frequent tumour types observed in *K14-Snail* animals was sebaceous gland carcinoma. Therefore, we first focused our analysis on the overall sebaceous gland morphology from the time of birth until the time of tumour formation. Staining for adipophilin, a lipid droplet-associated protein, showed that the composition of sebocytes in newborn *K14-Snail* mice was dramatically different from those observed in wild-type (*WT*) littermates (Figure 2a). Staining with the hyperproliferation marker Keratin-6 revealed that sebocytes expressing Snail were still highly proliferative when the mice were 3 weeks old, a time when normal terminal differentiation and cessation of sebocyte proliferation is observed in *WT* controls. Later on, the sebaceous gland cells in transgenic mice started to accumulate and several glands per hair follicle were formed (Figure 2b). This disorganisation was aggravated over time and led to sebaceous gland hyperplasia and carcinoma (Supplementary Figure S2). Sebaceous gland cells were disturbed in all *K14-Snail* mice, and this hyperproliferative behaviour and lack of terminal differentiation likely contributes to the high incidence of sebaceous gland carcinoma formation in the *K14-Snail* mice.

Given the peculiar morphology of sebaceous gland cells in *K14-Snail* mice, we screened a set of markers associated with sebaceous gland development and maintenance by qPCR analysis on RNA isolated from epidermis of newborn and adult mice (Supplementary Figure S3). This analysis revealed significant repression of the transcription factor Blimp-1 in *K14-Snail* mice ($P < 0.05$) (Figure 2c). A significant down-regulation of Blimp-1 reporter activity was observed in the sebocyte cell line SEB-1 and the breast cancer cell line MCF7 in transient Blimp-1 promoter assays (Figure 2d). Immunohistological analysis indeed confirmed the complete absence of Blimp-1 in the sebaceous gland of *K14-Snail* mice, whereas Blimp-1 expression still marked the terminally differentiated Snail-negative cells in the cornified layer (Figure 2e). Strikingly, Blimp-1-deficient mice show enhanced proliferation and expansion of the proliferative sebocyte pool.¹⁵ Consequently, by repressing Blimp-1, Snail contributes to the massive expansion of the sebaceous glands.

Snail expression results in aberrant FoxM1 activation and formation of aberrant spindle formation. Sebaceous gland cells are derived from stem cells from the bulge region.^{16–18} We next studied in detail both stem cells and progenitors present in this region. In contrast to newborn mice, in adult *K14-Snail* mice the Mts24-positive progenitor population was expanded and Mts24 was retained in some sebaceous gland cells (Figure 3a). Mts24 mRNA expression levels in adult *K14-Snail* mice were also significantly enhanced, reflecting the overall increased numbers of MTS24-expressing cells. In addition, the bulge stem cell

marker Lgr6 was reduced in these mice (Figure 3b). It is generally believed that clonogenic keratinocytes are closely related, if not identical, to multipotent stem cells. Therefore we compared the clonogenic capacity of CD34+ keratinocytes derived from *K14-Snail* mice with their *WT* counterparts at the age of 8 weeks: the *K14-Snail* cells formed many more and much larger colonies than the *WT* cells (Figure 3c). Mts24+ progenitors also have clonogenic potential.¹⁹ Again, we found the clonogenic potential significantly enhanced in Mts24+ cells isolated from the *K14-Snail* mice (Figure 3c). Microarray profiling of both stem cell and progenitor populations of *WT* and *K14-Snail* mice revealed the aberrant activation of FoxM1 and several downstream target genes²⁰ regulating cell cycle genes essential for G2/M progression, chromosomal segregation and cytokinesis (Figure 3d and Supplementary Figure S4). Aberrant activation of FoxM1 has been correlated with chromosomal instability.²¹ Consistent with this role, we found a high number of triple spindles in synchronised K38 keratinocyte cells stably transduced with Snail compared with control cells (Figure 3e).

Snail expression in keratinocytes promotes cell survival and resistance to genotoxic stress. To further understand the cellular role of Snail in skin tumourigenesis, and specifically its effect on cell survival and apoptosis, we isolated keratinocytes from newborn *WT* and *K14-Snail* mice. Treatment of the cells *in vitro* with the experimental genotoxic agent 2,4-dimethoxybenzaldehyde (DMBA) resulted in a clear survival advantage for keratinocytes expressing Snail compared with *WT* control cells (Figure 4a). At lower DMBA concentrations, *K14-Snail*-derived cells even showed enhanced proliferation in response to DMBA exposure. Treating the cells with the chemotherapeutic drug doxorubicin, which is used clinically to treat skin cancer patients, also led to a significant survival advantage for keratinocytes with transgenic Snail expression. Assessment of caspase-3 and -7 activities during both treatments demonstrated anti-apoptotic activity in cells expressing Snail (Figure 4a). We next investigated these findings further *in vivo* by using the classical DMBA/TPA (12-O-tetradecanoylphorbol-13-acetate) two-stage carcinogenic protocol, a treatment known to induce rapid development of skin papillomas. In line with a similar experiment,²² papilloma initiation was visible during week 8 of the TPA treatment. Single or multiple DMBA treatment without further promotion by TPA resulted in significantly more tumours in transgenic than in *WT* mice (Figure 4b). These experiments indicate that Snail expression on its own can synergise with DMBA treatment alone without the need for the tumour-promoting activity of TPA. As expected from macroscopic observations, the morphology of the tumours in *K14-Snail* transgenic mice looked different than the *WT* papillomas. There was a striking appearance of multiple infiltrating strands of cells spread all over the skin (Figure 4c) pointing to enhanced invasion. Cryosections stained with E-cadherin confirmed the histopathological analysis done with haematoxylin and eosin (H&E) staining: the dermis of DMBA-TPA-treated *K14-Snail* animals contained multiple small groups of epithelial cells. These cells stained E-cadherin weakly and were often E-cadherin negative (Supplementary Figure S5). Metastatic spread to

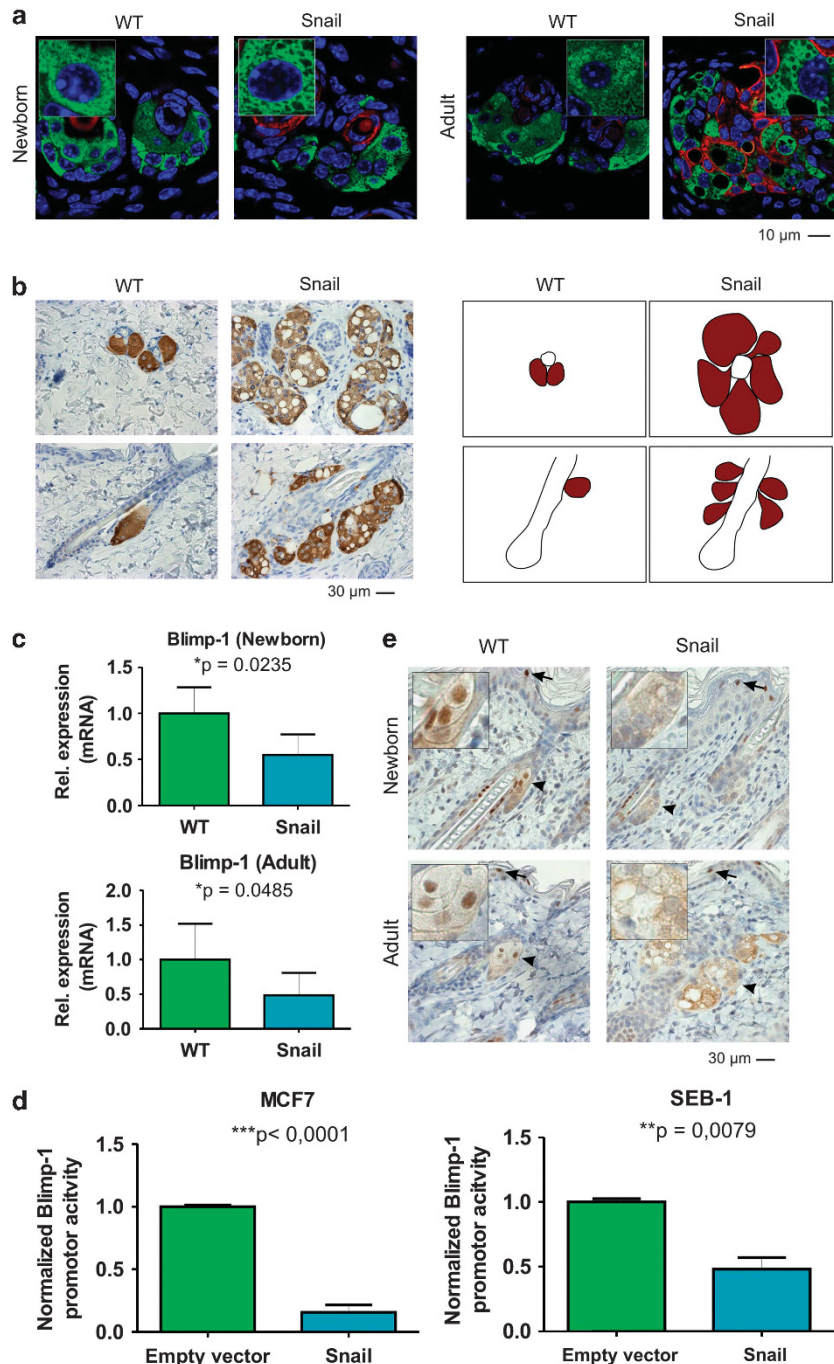


Figure 2 Snail expression leads to sebaceous gland hyperplasia and reduction of the transcription factor Blimp-1. (a) Confocal pictures of an immunohistological staining for adipophilin (green) and the hyperproliferation marker cytokeratin-6 (red) in WT and *K14-Snail* mice at the age of 6 days (left) and 3.5 weeks old (right) near the sebaceous gland (detail in insert— $3 \times$ magnified). (b) Adipophilin staining of skin sections of 4-month-old mice: transverse (upper panels) and longitudinal (lower panels) sections reveal the presence of many disorganised sebaceous gland islands in *K14-Snail* mice. (c) qPCR analysis reveals the strong reduction of Blimp-1 expression in *K14-Snail* mice compared with WT animals. Results are the average normalised relative expression values for four WT and four *K14-Snail* newborn mice and five WT and five *K14-Snail* adult mice. (d) *In vitro* analysis shows the significant reduction of Blimp-1 promoter activity in the presence of Snail expression in the sebocyte cell line SEB-1 (two independent experiments) and the breast carcinoma cell line MCF7 (three independent experiments). (e) Immunohistological analysis with an antibody-recognising Blimp-1 reveals the total absence of this transcription factor in the sebaceous gland of newborn and adult *K14-Snail* mice (presence in WT marked with arrowheads, and detail in insert— $3 \times$ magnified). However, the characteristic staining pattern in terminally differentiated keratinocytes in the suprabasal layer (marked by arrows) is retained

the lung, liver, spleen or peritoneum was not observed during the initial stages of these chemical carcinogenesis experiments. Overall, these data indicate that Snail, besides its role in tumour initiation, also contributes to cancer progression.

Tumour formation in Snail transgenic skin is accelerated in a p53 knock-out background. Given that keratinocytes from *K14-Snail* mice are more resistant to chemotoxic stress, we investigated the consequences of specifically inactivating

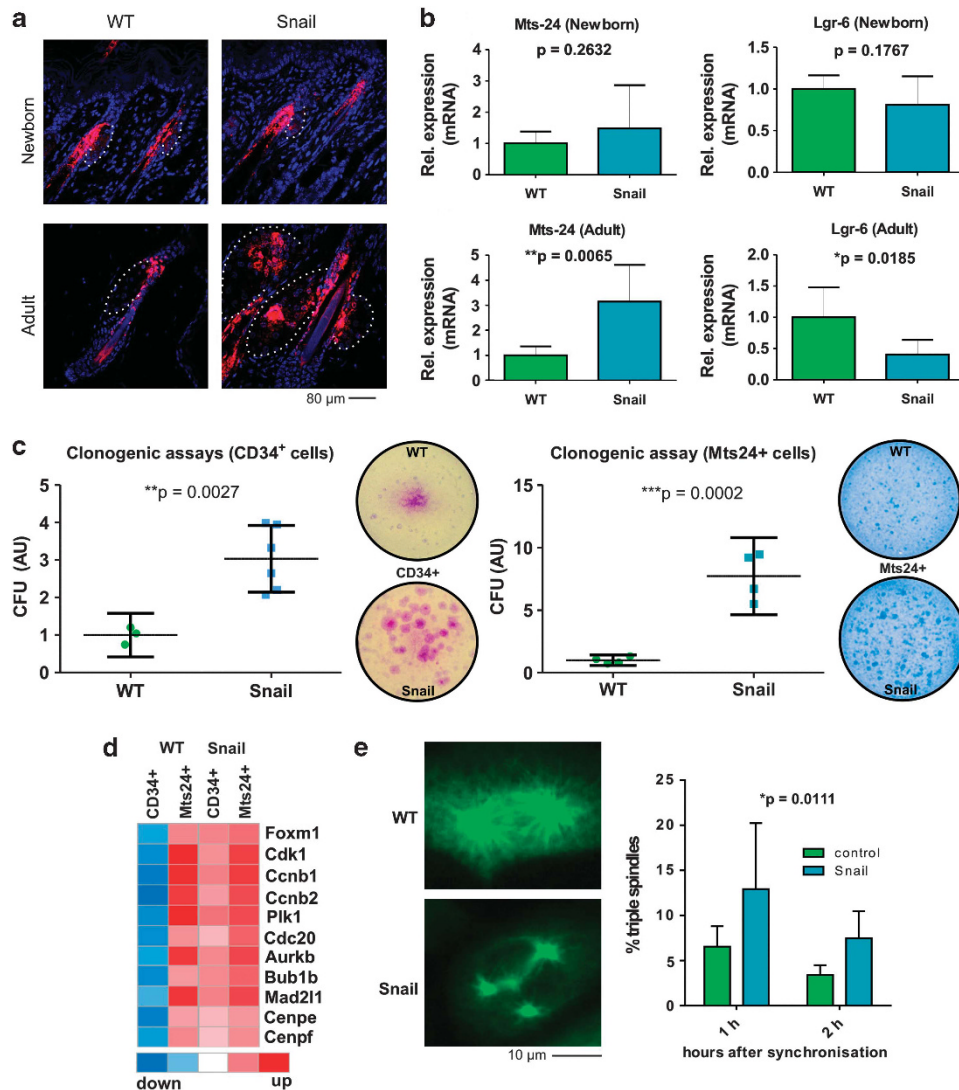


Figure 3 Snail expression enlarges the Mts24⁺ progenitor population and enhances the clonogenic capacity of CD34⁺ and Mts24⁺ cells. (a) Immunohistological staining for Mts24 in WT and K14-Snail mice (dotted lines mark the sebaceous gland boundaries). (b) qPCR analysis of Mts24 and Lgr6 expression in newborn and adult WT and K14-Snail epidermis. Results are the average normalised relative expression values for four WT and four K14-Snail newborn mice and five WT and five K14-Snail adult mice. (c) Clonogenic assay for CD34⁺ and Mts24⁺ keratinocytes from 8-week-old WT and K14-Snail mice. The relative number of colonies resulting from seeding equal numbers of CD34⁺ keratinocytes from WT ($n = 3$) and K14-Snail ($n = 6$) mice and of Mts24⁺ keratinocytes from WT ($n = 4$) and K14-Snail ($n = 4$) mice, 95% confidence intervals are indicated. Representative image showing that colonies of CD34⁺ and Mts24⁺ selected cells are larger in number and size in K14-Snail mice than in WT controls. (d) Microarray analysis for CD34⁺ and Mts24⁺ keratinocytes from 8-week-old WT and K14-Snail mice reveals an aberrant activated FoxM1 pathway in K14-Snail CD34⁺ stem cells. (e) A proportion of dividing stable keratinocyte cells (K38) show triple spindles when overexpressing Snail compared with luciferase control cells as shown by an alpha-tubulin staining (left). Quantification of the number of triple spindles 1 and 2 h after synchronisation of K38 cells with thymidine and nocodazole ($n = 5$) (right)

p53 in the skin. p53 is an important tumour suppressor that eliminates cells subjected to different forms of stress, including those exposed to DMBA/TPA protocols. We genetically intercrossed the K14-Snail mice with a tissue-specific knockout of p53, K14Cre;Trp53^{fl/fl}.²³ Although K14-Snail;K14Cre;Trp53^{fl/fl} mice do not develop significantly more tumours than K14-Snail mice alone (Figure 5a), tumourigenesis is much more rapid, with a median latency of 176 days (Supplementary Table SI). This finding indicates that expression of Snail and loss of p53 synergise in initiating tumours, probably by allowing cells with damaged DNA to survive. In addition to the different histological subtypes of

spontaneous skin tumours observed in the K14-Snail mice, K14-Snail;K14Cre;Trp53^{fl/fl} mice also developed more aggressive carcinosarcomas characterised by the biphasic appearance of intermixed epithelial and mesenchymal elements (Supplementary Tables SI, SII and Figure 5b).

Snail expression drives malignant skin cancer progression. Aberrant expression of Snail in epithelial cancer cell lines has been reported to endow cells with enhanced invasive properties, which could contribute to the formation of metastases.²⁴ Sebaceous gland carcinomas in K14-Snail mice were the most highly metastatic, as draining

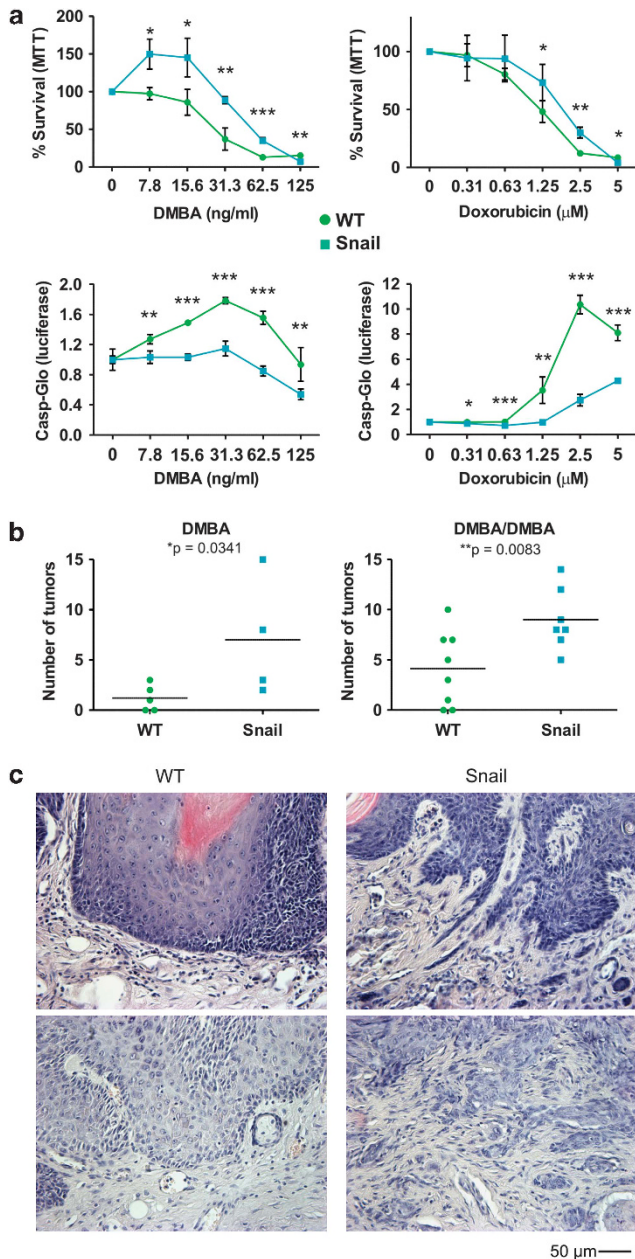


Figure 4 Snail expression enhances cell viability and confers resistance to apoptosis. (a) Primary keratinocytes of pups from *WT* and *K14-Snail* animals were isolated and treated with different concentrations of DMBA (left panels) or doxorubicin (right panels). Survival was measured with an MTT assay (upper panels), and the results are presented as the average of three independent experiments of treated pooled keratinocytes from at least two different mice. Apoptosis was measured with a caspase-3/7 Glo assay, and the results are presented as the average of two experiments of treated pooled keratinocytes from at least two different mice. (* $P < 0.05$, ** $P < 0.01$, *** $P < 0.001$). (b) Skin carcinogenesis in *WT* and *K4-Snail* mice after single (left) or multiple (right) DMBA treatments. The number of skin papillomas per mouse is shown. (c) Immunohistological analysis of the skin of DMBA-treated mice reveals highly invasive regions in *K14-Snail* animals but not in *WT* controls. Upper and lower panel shows the histology of two independent tumours with H&E staining

lymph nodes of 59% of transgenic mice with sebaceous gland carcinomas contained carcinoma cells with sebaceous differentiation (Figure 5c). Given that metastasis of malignant

tumours to regional lymph nodes is one of the earliest signs of cancer spread in patients,²⁵ we histologically examined different other organs, but we could not observe distant metastasis of sebaceous cancer cells. However, we found lung metastasis displaying features of terminal skin differentiation in mice with primary tumours resembling SCCs (Supplementary Figure S6 and Figure 5c). As *K14Cre;Trp53^{fl/fl}* mice form spontaneous benign skin tumours that are non-metastatic, they are suitable for investigating the phenotypic consequences of additional mutations in genes implicated in tumour progression and metastasis. Indeed, Kaplan–Meier survival analysis indicates that Snail drives malignant progression even further as was evidenced by the overall statistically significant difference between the survival curves. Moreover, in contrast to the *K14Cre;Trp53^{fl/fl}* mice, *K14-Snail;K14Cre;Trp53^{fl/fl}* mice formed aggressive carcinosarcomas, which are highly invasive, again pointing to the contribution of the Snail nuclear protein to enhancing malignancy in synergy with p53 deficiency.

Discussion

In vitro evidence for the involvement of Snail in cancer progression has been increasing. However, little is known about the molecular mechanism of Snail's contribution to the early onset of epithelial cancer *in vivo* and particularly its role in skin cancer progression. Therefore, we studied the cellular and molecular consequences of Snail expression in the basal layer of the skin.

K14-Snail mice develop spontaneous skin tumours of different histological subtypes, of which sebaceous gland carcinoma is one of the most prominent. In the sebaceous compartment, we have observed a continuous expansion of a population of cells leading to sebaceous hyperplasia and eventually sebaceous carcinoma with metastatic spread to the lymph nodes. The intense sebocyte proliferation and glandular growth can be explained by the continuous proliferation and expansion of the enlarged Mts24 + progenitor population and the loss of Blimp-1-positive sebaceous cells. The transcriptional repressor Blimp-1 marks the terminally differentiated region of the sebaceous gland.²⁶ We found that loss of Blimp-1 in the sebaceous gland is one of the earliest molecular consequences of Snail expression in the skin. Furthermore, SCD3, another marker for terminal sebocyte differentiation, was downregulated in *K14-Snail* mice compared with *WT* mice (data not shown). Snail directly represses Blimp-1 promoter activity in the sebocyte cell line SEB-1. In agreement with our findings, conditional Blimp-1 ablation in the skin results in enhanced sebocyte proliferation.¹⁵ Collectively, these data indicate that the gatekeeper of sebaceous gland homeostasis, Blimp-1, is a direct target of Snail.

In addition to sebaceous gland carcinoma development, we also observed tumours resembling BCCs. We were able to show local, Snail-positive regions in a subset of human BCCs. Complementary to our data, conditional expression of Gli1 in mouse skin induces hyperplastic lesions evolving into BCC.²⁷ In these mice, Snail transcripts were detected as an early response to enhanced Gli1 activity, suggesting that Snail could functionally contribute to tumour initiation. Moreover, our data indicate that Snail is not only implicated in the early

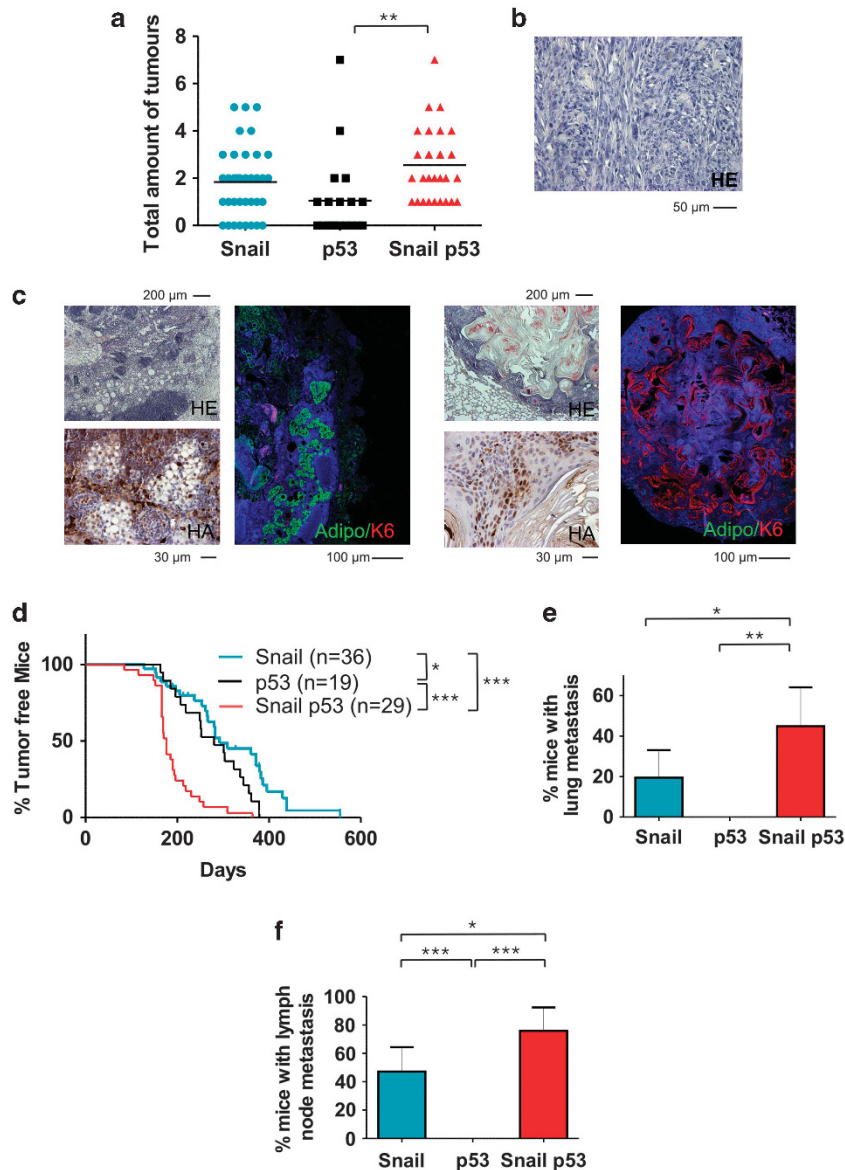


Figure 5 Synergistic effects of combining Snail expression with loss of the p53 tumour suppressor *in vivo*. (a) *K14-Snail;K14Cre;Trp53^{fl/fl}* mice have on average more skin tumours than *K14-Snail* and *K14Cre;Trp53^{fl/fl}* mice. (b) Histological analysis with a H&E staining reveals carcinosarcoma as an additional tumour type in *K14-Snail;K14Cre;Trp53^{fl/fl}* mice. (c) (Left panel) Metastasis to lymph nodes was detected in *K14-Snail* mice: histological analysis with H&E staining shows cells with sebaceous characteristics (upper left); these cells stain positive for HA-tagged Snail (lower left). The infiltrating cells have retained the sebaceous cell marker adipophilin (green); no expression of the proliferation marker K6 (red) is observed. (Right panel) Metastasis to lungs was observed in *K14-Snail* mice. The nodules show a high degree of keratinisation (upper left) and are partially positive for HA-tagged Snail (lower left). The nodules are strongly K6-positive (red) but do not express adipophilin (green) (left). (d) Kaplan–Meier tumour-free survival curves for *K14-Snail*, *K14Cre;Trp53^{fl/fl}* and *K14-Snail;K14Cre;Trp53^{fl/fl}* mice. (e) Incidence of lung metastasis in mice with skin tumours. Bars represent 95% confidence intervals. (f) Incidence of lymph node metastasis in mice with skin tumours. Bars represent 95% confidence intervals. (Statistical significance used in this figure: * $P < 0.05$, ** $P < 0.01$, *** $P < 0.001$)

onset of the tumours but also contributes to invasiveness, as has been observed in a subset of human BCCs. Finally, we found cutaneous SCC among the spontaneous tumours that arose in *K14-Snail* mice. This common cancer typically arises from malignant proliferation of keratinocytes in the epidermis and is characterised by invasive growth and presence of keratin pearls. It was previously demonstrated that Snail knockdown in the squamous carcinoma HaCa4 cell line has a large effect on cellular invasiveness, tumour growth and metastasis.²⁸ In contrast to BCC, SCC can metastasise in

humans. Indeed, in mice with primary SCCs we identified metastatic lung nodules displaying distinct features of skin differentiation. This is a strong indicator that the cancer dissemination is fuelled by Snail-expressing cancer stem cells derived from the skin, which have not lost their ability to establish organised structures at distant sites. Likewise, it has been proposed that in colorectal cancer EMT is involved in primary tumour progression and that subsequent redifferentiation (MET) takes place towards an epithelial phenotype in metastases.²⁹

Skin is a very plastic organ and several of its cell populations seem to have stem cell properties.³⁰ Both CD34+ and Mts24+ keratinocytes derived from *K14-Snail* mice have a much higher clonogenic potential than *WT* keratinocyte stem cell populations, leading us to conclude for the first time that Snail has an important role *in vivo* in the expansion of stem cell and progenitor cell populations that lack the ability to terminally differentiate normally, explaining sebaceous gland hyperplasia and eventually sebaceous gland carcinoma in *K14Snail* mice. However, given the different tumour types that we have observed we postulate Snail involvement in distinct activated stem cell populations. Although it has been shown that differentiated epithelial breast cell lines acquire cancer stem cell characteristics such as the ability to grow in semi-solid medium and form mammospheres when they express Snail,³¹ we here provide the first *in vivo* evidence for the oncogenic potential of Snail to enhance the CD34+ cancer stem cell population of the skin. It is clear as well from our analysis that Snail activates FoxM1 expression and its downstream target genes. It has been shown that FoxM1 upregulation induces genomic instability in epidermal keratinocytes.²¹ We also show that cells expressing Snail in a malignant context have an increased resistance to genotoxic and other forms of stress. This survival advantage has been previously demonstrated in the recurrence of breast cancer accompanied by an EMT phenotype and strong expression of Snail.^{7,32} Moreover, Snail expression results in increased radioprotection in transgenic CombitTA-Snail mice.³³ These observations are complementary to our data here in the skin demonstrating that Snail-expressing keratinocytes are more resistant to apoptosis, and that they even gain a proliferative advantage when subjected to chemical carcinogens or chemotherapeutics. Consequently, *K14-Snail* mice form more tumours when subjected not only to the classical DMBA/TPA protocols, which confirms the observations of Due *et al.*,²² but also when subjected to one or more DMBA treatments without further promotion. This is a very strong indicator that Snail maintains the proliferation and tumour-promoting activity necessary for the expansion of the initiated cells during tumour promotion.

The tumour-suppressor p53 has an integral role in cellular responses to DNA damage, but there is also substantial evidence that p53 deficiency facilitates reprogramming of differentiated cells.³⁴ Moreover, p53 loss rescues epidermal stem cell function in telomerase-deficient mice.³⁵ In *K14-Snail; K14Cre; Trp53^{fl/fl}* mice, we found not only the tumour types observed in *K14-Snail* mice, but carcinosarcomas as well, which is an indication of greater plasticity observed through the combined loss of p53 and Snail overexpression. Our data suggest that the combination of Snail expression and loss of p53 is probably an important trigger for this tumour type that may also potentially need the accumulation of additional critical mutations. Besides the formation of carcinosarcomas in *K14-Snail; K14Cre; Trp53^{fl/fl}* mice, tumour onset and lung metastasis were dramatically enhanced. The increase in lung metastases in this combinatorial model may also be due not only to a more rapid outgrowth of lung micrometastasis but also to lung nodules arising from the carcinosarcomas, which are a much more aggressive tumour than those formed by increased metastasis of SCCs.

In summary, our data show that expression of the transcriptional repressor Snail is involved in the onset and progression of tumour formation in skin at several different levels (see Summary model in Figure 6). At onset, Snail expression affects the *in vivo* proliferative capacity of keratinocytes leading to a block in the terminal differentiation of specific sub-populations of progenitors, such as Blimp-1 as direct target in sebocytes. We have demonstrated for the first time *in vivo* that Snail expression in addition to its role in EMT is also linked to the expansion of CD34+ stem cell populations in the skin through *ex vivo* clonogenic assays. In addition, as populations of non-terminally differentiated cells accumulate genetic mutations, for example, by aberrant activation of FoxM1, Snail appears to lead to intrinsic protection of these cells that allows their survival and further accumulation of genomic aberrations allowing the progression to carcinoma. At this stage, Snail's widely reported *in vitro* function as inducer of EMT comes into play enabling the cells to invade and migrate, which eventually leads to metastasis.

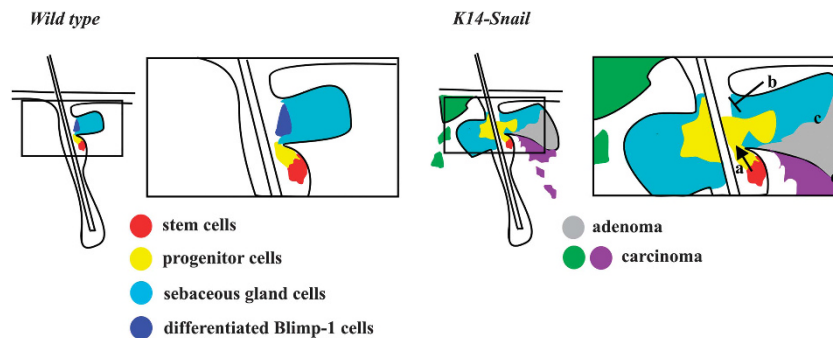


Figure 6 Summary model: Snail expression drives skin cancer progression. (Left) *WT* overview and detail map of the skin regions of interest studied here in more detail: bulge region containing CD34+ stem cells (red), progenitor region containing Mts24+ progenitor cells (yellow), and sebaceous gland region (blue) with terminally differentiated Blimp-1+ cells (dark blue). (Right) (a) At onset, Snail expression certainly can affect the *in vivo* proliferative capacity of keratinocyte stem cells, leading to the expansion of the Mts24+ progenitor region and (b) the block in their terminal differentiation. (c) Snail acts as a survival factor in non-terminally differentiated cells accumulating genetic aberrations (stress, mutations) allowing (d) progression to carcinoma. Snail acts at this stage as EMT inducer enabling the cells to invade and migrate, which eventually leads to metastasis

Material and Methods

Tumour analysis. Experiments were done in accordance with the institutional guidelines regarding the care and use of laboratory animals. *K14-Snail*, *K14Cre;Trp53^{fl}* and *K14-Snail;K14Cre;Trp53^{fl}* mice were killed as soon as the spontaneous tumours reached 15 mm³ or sooner if they were suffering from tumour burden. Tumours and organs were either snap-frozen in liquid nitrogen for further analysis or fixed in 4% paraformaldehyde, processed and embedded in paraffin for histological studies. H&E or antibody staining on paraffin sections were carried out using standard procedures as described below. Tumours were scored and classified independently by two scientists, and their consensus is presented in the tables. Human tumour biopsies were obtained from surgical excisions of the affected areas at the Department of Dermatology, University of Cologne, Cologne, Germany. The patients signed the informed consent from the Department of Dermatology, University of Cologne, approved by the Institutional Commission of Ethics (Az.08-144). The study was conducted according to the Declaration of Helsinki Principles. The tumour data set contain 30 BCCs, 6 poroma/porocarcinomas, 4 sebaceous gland carcinomas and 2 trichoblastomas. In addition, we stained four microcystic adnex carcinomas, three melanomas and two trichoepitheliomas, which all turned out to be Snail negative.

Carcinogenesis protocols. Experiments were done in accordance with the institutional guidelines regarding the care and use of laboratory animals. For two-stage chemical carcinogenesis, we shaved the backs of 8-week-old mice using a Wella Contoura hair clipper (Wella, Bio Services, Uden, The Netherlands) and treated them 2 days later with a single application of DMBA (25 µg in 200 µl acetone) (Sigma, Diegem, Belgium; cat. no. D-3254). One week later, we started biweekly applications of TPA (200 µl of 10⁻⁴ M solution in acetone) (Fluka, Sigma, cat. no. 79346) for 12 weeks. We visually examined the mice weekly. Mice were shaved in week 3 and week 6 (before papilloma formation) to allow better distribution of the chemicals on the skin. Ten WT and ten Snail transgenic littermates were treated with the DMBA/TPA protocol. Another five mice got only DMBA treatment and were treated further only with the vehicle, acetone. In addition, eight mice were treated with DMBA two times per week for 8 weeks. Two WT mice and two *K14-Snail* transgenic mice were treated with acetone both at the initiation step and in the subsequent promotion steps. Tumours and organs were processed as described above.

Immunohistochemistry. Tumours and organs were isolated and fixed overnight in 4% paraformaldehyde solution, processed and cut into 6-µm sections. For histology, samples were stained with H&E. For immunohistochemical staining, antigen retrieval was done in citrate buffer and endogenous peroxidases were blocked with 3% H₂O₂. The sections were incubated with primary antibodies and stained with biotin-conjugated secondary antibodies followed by Streptavidin-HRP (substrate development with DAB) or Streptavidin Alexa Fluor. When necessary, the signal was amplified using the Tyramide Signal Amplification (TSA) kit (Perkin Elmer, Zaventem, Belgium).

The following antibodies were used: mouse anti-Snail (1/80),¹⁴ mouse anti-HA-tag (1/1000) (Babco, Eurogentec, Seraing, Belgium; cat. no. MMS-101R), rat anti-Ki-67 (1/30) (Dakopatts, Dako Belgium, Leuven, Belgium; cat. no. M 7249), rabbit anti-Blimp-1 (1/3000),³⁶ guinea pig anti-adipophilin (1/3000) (Fitzgerald Industries International, Concord, MA, USA; cat. no. RDI-PROGP40), rat anti-E-cadherin (1/1000) (Sigma U-3254), rabbit anti-cytokeratin 14 (1/3000) (Babco/Covance Res. Prod., Eurogentec, cat. no. PRB-155P), rabbit anti-filaggrin 14 (1/1000) (Babco/Covance Res. Prod. cat. no. PRB-417P), rabbit anti-involucrin 14 (1/5000) (Babco/Covance Res. Prod. cat. no. PRB-140C) rat anti-Plet-1 (1/60)³⁷ and mouse anti-alpha-tubulin antibody (1/100) (Pierce, Fisher Scientific, Doornik, Belgium; MA1-19162).

Keratinocyte culture. Pups were decapitated at the age of 2 days, and their limbs and tail were removed. A tail tip was kept aside for genotyping. The body was subsequently disinfected in isobetadine and washed twice in 70% ethanol and three times in PBSA containing 250 µg/ml gentamycin. The skin was carefully dissected and incubated for at least 30 min in PBSA containing 250 µg/ml gentamycin. The skins were spread in a petridish (dermis down), and sufficient dispase II solution was added to allow the skins to float on the solution. Dispase II solution was prepared by dissolving 2.5 U/ml dispase II in Ca²⁺-free keratinocyte medium (Clonetics, Lonza, Verviers, Belgium; cat. no. CC-3112) without serum. After overnight incubation at 4 °C, the dispase II solution was removed, and the epidermis was separated from dermis. The epidermis was cut in pieces and

incubated for 10 min in a 5 × trypsin/EDTA solution (Gibco, Life Technologies, Gent, Belgium; cat. no. 15400-054, diluted in PBSA) at 37 °C on a rotation wheel. The tubes were shaken vigorously to dissociate the cells from clumps. FCS was added to the suspension, and the cells were filtered through 70-µm strainers to remove the remaining clumps. Cells were centrifuged (7 min at 1250 r.p.m.), resuspended in Ca²⁺-free keratinocyte medium with 10% FCS, centrifuged again (7 min at 1250 r.p.m.) and resuspended in Ca²⁺-free keratinocyte medium with 10% FCS. The cells were counted, plated at 1.4 × 10⁵ cells/cm² and incubated at 37 °C in a humidified incubator with 5% CO₂. The next day, the medium was replaced with Ca²⁺-free keratinocyte medium without serum. The cells were maintained by changing the medium every second day with Ca²⁺-containing keratinocyte medium (Clonetics cat. no. CC-3111). Genotyping of pups was done with specific sequences spanning the HA-tagged region of the Snail sequence: forward primer 5'-CGGCGCGTCGTCCTCTCG-3' and reverse primer 5'-ACGCATAATCTGGTACATCATAA-3'.

Preparation of keratinocytes of adult mice followed the same procedure, with slight modifications: the back skins of adult mice were incubated overnight on a 1 × trypsin solution (Gibco BRL cat. no. 25050-014) instead of dispase II solution, and incubation in trypsin/EDTA at 37 °C on a rotation wheel was omitted from the following steps. For clonogenic assays, we followed a published protocol.³⁸ CD34-positive cells were selected with a biotinylated CD34 antibody (eBioscience, Vienna, Austria; cat. no. 13-0341-85) using the easySEP mouse biotin kit (Stem Cell Technologies, Grenoble, France; cat. no. 18556) and easySEP magnet (Stem Cell Technologies, cat. no. 18000) following the manufacturer's instructions. Mts24-positive cells were selected using a specific antibody³⁷ followed by incubation with an anti-rat PE-labelled secondary antibody (BD Biosciences, Becton Dickinson Benelux, Erembodegem, Belgium; cat. no. 550767). Cells were then purified further using the easySEP mouse PE kit (Stem Cell Technologies cat. no. 18554) and easySEP magnet, following the manufacturer's instructions. Cells from WT and *K14-Snail* mice were seeded at equal densities on 3T3J2 feeder layers and maintained in custom DMEM:Ham F12 medium (3:1) without Ca²⁺ (Genaxxon, Ulm, Germany) for 2 weeks at 32 °C in 8% CO₂. Cells were fixed with 4% paraformaldehyde and stained with a 1% Nile blue (Sigma cat. no. N-5632) and 1% Rhodamine B (Sigma cat. no. R-6626) solution.

Microarray analysis. Keratinocytes from 8-week-old WT and *K14-Snail* mice were sorted for CD34 and Mts24 as described above. RNA was prepared with TRIsure (Bioline, GC Biotech, Alphen aan den Rijn, The Netherlands; cat. no. BIO-38032), and after quality check with the NanoDrop spectrophotometer and the Agilent 2100 Bioanalyser, Affymetrix mouse gene 1.0 ST arrays were hybridised following the manufacturer's instructions at the Nucleomics VIB facility (Leuven, Belgium). Data analysis comprised looking for differentially expressed genes (at least two-fold) between positive versus negative fractions for CD34 and Mts24 for both WT and *K14-Snail* mice. Differentially expressed genes were imported into IPA (Ingenuity Systems, Redwood City, CA, USA) to uncover the underlying modulated pathways.

Real-time qPCR analysis. RNA was extracted from *K14-Snail* and WT control mice at the ages of 4 days ($n=4$) and 4 months ($n=5$) as follows. Mice were killed by cervical dislocation, and the hair was removed from old mice using a Wella Contoura hair clipper. Skin was dissected from the back and incubated the dermis down on 0.5 M ammonium thiocyanate (Sigma-Aldrich cat. no. 431354) for 30 min at 37 °C. Epidermis was then easily separated from the dermis. Epidermis was diced into very small pieces using sterile scalpels and transferred to TRIsure (Bioline cat. no. BIO-38032), shaken very well and centrifuged at maximum speed in a table-top centrifuge.

RNA was extracted from the supernatant according to the manufacturer's instructions. RNA was treated with 1 U of RNase-free DNase RQ1 (Promega, Leiden, The Netherlands; cat. no. M6101) per 1 µg RNA for 30 min at 37 °C in appropriate buffer. DNase was inactivated by incubation in Promega's stop solution for 10 min at 65 °C. Bulk Mg²⁺ was removed by using Amicon ultra 0.5-ml centrifugal filters (Millipore, Brussels, Belgium; cat. no. UFC510096) in two consecutive diluting washes. cDNA synthesis was performed with iScript (Bio-Rad, Eke, Belgium; cat. no. 170-8891) following the manufacturer's instructions.

Quantitative PCR was done using the Fast SYBR master mix kit (Applied Biosystems, Life Technologies, Gent, Belgium; cat. no. 4385618) for the genes of interest and reference genes Rpl13a and Actb. Primers were designed using Primer Express 1.0 Software (Perkin Elmer; Applied Biosystems). Plates were run on the LightCycler 480 (Roche, Vilvoorde, Belgium). The average threshold cycle of

triplicate reactions was used for all subsequent calculations using the deltaC_T method. Graphs represent the average normalised relative expression values of *K14-Snail* and *WT* mice, with the *WT* average normalised relative expression value at 4 days set to 1. The following primer sequences were used in this study: Blimp-1 forward 5'-CAGAGCCGAGTTTGAAGAGA-3', reverse 5'-AAGGATGCCTCGGCTTGAA-3'; Mts24 forward 5'-CCCAAAGCCAGTCGGTCTT-3', reverse 5'-GTGCGATTGACGACGATGAG-3'; Lgr6 forward: 5'-AGGGAACCTGGCCCTGTCTC-3', reverse 5'-GGATGAAAGTCCTCGGCCTG-3'; Rpl13a forward 5'-CCGTGCTCTCAAGGTGTT-3', reverse 5'-TGGTTGTCACTGCCTGGTACTT-3'; and Actb forward 5'-GCTTCTAGCGGACTGTTACTGA-3', reverse 5'-GCCATGCCAATGTTGTCTTAT-3'.

In vitro assays. Keratinocytes cultured for 3 days in 24-well plates were treated with different concentrations of DMBA (Sigma cat. no. D-3254) or doxorubicin (Sigma cat. no. D-1515) (quadruplicates) as indicated in the Results section. For the proliferation assay with MTT, the medium was refreshed 2 days after treatment, and MTT stock solution (5 mg/ml, dissolved in PBSA) (Sigma cat. no. M-2128) was added (1/5 ratio MTT solution to medium). Plates were incubated for 2 h at 37 °C. After discarding the supernatant, DMSO was added to the wells and pipetted up and down several times to allow the converted dye to dissolve completely. The solution was transferred to a 96-well plate for measurement in a Benchmark microplate reader (Bio-Rad) at 595 nm with background subtraction at 655 nm. Caspase activity was measured with Caspase-Glo 3/7 assay (Promega cat. no. G8092) 1 day after treatment, following the manufacturer's protocol.

Generation and synchronisation of K38 cells. K38 cells (stable primary mouse keratinocytes) were maintained as described.³⁹ Cells were transduced with lentiviral constructs allowing expression of Snail (pdWPI-mSnail) or luciferase (pdWPI-Luc) and sorted for EGFP to have a homogeneous expressing population. Cells were synchronised with thymidine–nocodazole (mitotic block): cells were treated for 24 h with 2 mM thymidine (Sigma cat. no. T9250), washed with PBS salt solution and allowed to be released from S-phase block by incubation in regular medium for 3 h. Next, cells were treated with nocodazole (10 ng/ml medium) (Sigma cat. no. M1404) for 12 h. Cells were washed with PBS and incubated in regular medium to allow their release.

Statistical analysis. Data analysis was performed using the GraphPad Prism 5 software (La Jolla, CA, USA).

Reporter assays. Transient transfection of SEB-1⁴⁰ and MCF7 cell lines was performed using the FuGENE6 reagent (Roche cat. no. 1814443). Cells were seeded the day before transfection (40 000 cells/well in a 24-well plate). Cells were transiently transfected with the 1921 bp upstream Blimp-1 promoter sequence followed by a luciferase reporter (p1921)⁴¹ and co-transfected with an expression plasmid for hSnail (pEF6-hSnail) or an empty vector control (pEF6/myc-His A (Invitrogen, Life Technologies, Gent, Belgium). Lysates for further analysis were made 96 h after transfection using GalactoStar lysis buffer (Tropix, Life Technologies, Gent, Belgium; cat. no. T1014). Luciferase activity was measured using a luciferase substrate buffer (40 mM Tricine, 2.14 mM (MgCO₃)₄Mg(OH)₂·5H₂O, 5.34 mM MgSO₄·7H₂O, 66.6 mM DTT, 0.2 mM EDTA; the solution was filtered through a Millipore glass filter. Then we added 521.2 μM coenzyme A, 734 μM ATP and 940 μM luciferase. Transfection normalisation was done by measuring beta-galactosidase (GalactoStar kit, Tropix), which was encoded by cotransfected plasmids containing a beta-actin and RSV promoter upstream of a LacZ cassette.

Conflict of Interest

The authors declare no conflict of interest.

Acknowledgements. We thank Professor Jody J Haigh and Dr. Amin Bredan for critical reading of the manuscript and the members of our research group for valuable discussions. We thank Professor D Thiboutot for providing the SEB-1 cell line, Dr. K Wright for providing the Blimp-1 reporter construct, Dr. R. Tooze for providing the Blimp-1 antibody, Dr. A Sonnenberg for the Mts24 antibody and Dr. J Reichelt for the K38 cells. We also thank S. Noppen (the DMBR microscopy core) for the help with microscopic analysis. This research was funded by grants from the FWO, the Geconcerteerde Onderzoeksacties of Ghent University, the Stichting tegen Kanker, the Association for International Cancer Research

(Scotland), the EU-FP6 framework program BRECOSM LSHC-CT-2004-503224, the EU-FP7 framework program TuMIC 2008-201662 and the Deutsche Forschungsgemeinschaft (SFB 829, Z2, to CM).

Author Contributions

BDC, GD, PV and JT performed the experiments and analysed the interpreted data. CM, AD, JJ and EF provided valuable reagents/material. BDC and GB conceived and designed the project, analysed the interpreted data and wrote the paper with inputs from all authors.

- Friedl P, Wolf K. Tumour-cell invasion and migration: diversity and escape mechanisms. *Nat Rev* 2003; **3**: 362–374.
- De Craene B, Bex G. Regulatory networks defining EMT during cancer initiation and progression. *Nat Rev* 2013; **13**: 97–110.
- Cano A, Perez-Moreno MA, Rodrigo I, Loscascio A, Blanco MJ, del Barrio MG *et al*. The transcription factor snail controls epithelial-mesenchymal transitions by repressing E-cadherin expression. *Nat Cell Biol* 2000; **2**: 76–83.
- Battle E, Sancho E, Franci C, Dominguez D, Monfar M, Baulida J *et al*. The transcription factor snail is a repressor of E-cadherin gene expression in epithelial tumour cells. *Nat Cell Biol* 2000; **2**: 84–89.
- De Craene B, Gilbert B, Stove C, Bruyneel E, van Roy F, Bex G. The transcription factor snail induces tumor cell invasion through modulation of the epithelial cell differentiation program. *Cancer Res* 2005; **65**: 6237–6244.
- Moreno-Bueno G, Cubillo E, Sarrío D, Peinado H, Rodriguez-Pinilla SM, Villa S *et al*. Genetic profiling of epithelial cells expressing E-cadherin repressors reveals a distinct role for Snail, Slug, and E47 factors in epithelial-mesenchymal transition. *Cancer Res* 2006; **66**: 9543–9556.
- Moody SE, Perez D, Pan TC, Sarkisian CJ, Portocarrero CP, Sterner CJ *et al*. The transcriptional repressor Snail promotes mammary tumor recurrence. *Cancer cell* 2005; **8**: 197–209.
- Olmeda D, Moreno-Bueno G, Flores JM, Fabra A, Portillo F, Cano A. SNAI1 is required for tumor growth and lymph node metastasis of human breast carcinoma MDA-MB-231 cells. *Cancer Res* 2007; **67**: 11721–11731.
- Fraga MF, Herranz M, Espada J, Ballestar E, Paz MF, Ropero S *et al*. A mouse skin multistage carcinogenesis model reflects the aberrant DNA methylation patterns of human tumors. *Cancer Res* 2004; **64**: 5527–5534.
- Li X, Deng W, Lobo-Ruppert SM, Ruppert JM. Gli1 acts through Snail and E-cadherin to promote nuclear signaling by beta-catenin. *Oncogene* 2007; **26**: 4489–4498.
- Hoot KE, Lighthall J, Han G, Lu SL, Li A, Ju W *et al*. Keratinocyte-specific Smad2 ablation results in increased epithelial-mesenchymal transition during skin cancer formation and progression. *J Clin Invest* 2008; **118**: 2722–2732.
- Jamora C, Lee P, Kociniowski P, Azhar M, Hosokawa R, Chai Y *et al*. A signaling pathway involving TGF-beta2 and snail in hair follicle morphogenesis. *PLoS Biol* 2005; **3**: e11.
- Becker KF, Rosivatz E, Blechschmidt K, Kremmer E, Sarbia M, Hofler H. Analysis of the E-cadherin repressor Snail in primary human cancers. *Cells Tissues Organs* 2007; **185**: 204–212.
- Franci C, Takkunen M, Dave N, Alameda F, Gomez S, Rodriguez R *et al*. Expression of Snail protein in tumor-stroma interface. *Oncogene* 2006; **25**: 5134–5144.
- Horsley V, O'Carroll D, Tooze R, Ohinata Y, Saitou M, Obukhanych T *et al*. Blimp1 defines a progenitor population that governs cellular input to the sebaceous gland. *Cell* 2006; **126**: 597–609.
- Morris RJ, Liu Y, Marles L, Yang Z, Trempe C, Li S *et al*. Capturing and profiling adult hair follicle stem cells. *Nat Biotechnol* 2004; **22**: 411–417.
- Oshima H, Rochat A, Kedzia C, Kobayashi K, Barrandon Y. Morphogenesis and renewal of hair follicles from adult multipotent stem cells. *Cell* 2001; **104**: 233–245.
- Snippert HJ, Haeghebarth A, Kasper M, Jaks V, van Es JH, Barker N *et al*. Lgr6 marks stem cells in the hair follicle that generate all cell lineages of the skin. *Science* 2010; **327**: 1385–1389.
- Nijhof JG, Braun KM, Giangreco A, van Pelt C, Kawamoto H, Boyd RL *et al*. The cell-surface marker MTS24 identifies a novel population of follicular keratinocytes with characteristics of progenitor cells. *Development* 2006; **133**: 3027–3037.
- Laoukili J, Kooistra MR, Bras A, Kaur J, Kerkhoven RM, Morrison A *et al*. FoxM1 is required for execution of the mitotic programme and chromosome stability. *Nat Cell Biol* 2005; **7**: 126–136.
- Teh MT, Gemenetidis E, Chaplin T, Young BD, Philpott MP. Upregulation of FOXM1 induces genomic instability in human epidermal keratinocytes. *Mol Cancer* 2010; **9**: 45.
- Du F, Nakamura Y, Tan TL, Lee P, Lee R, Yu B *et al*. Expression of snail in epidermal keratinocytes promotes cutaneous inflammation and hyperplasia conducive to tumor formation. *Cancer Res* 2010; **70**: 10080–10089.
- Jonkers J, Meuwissen R, van der Gulden H, Peterse H, van der Valk M, Berns A. Synergistic tumor suppressor activity of BRCA2 and p53 in a conditional mouse model for breast cancer. *Nat Genet* 2001; **29**: 418–425.
- Thiery JP, Acloque H, Huang RY, Nieto MA. Epithelial-mesenchymal transitions in development and disease. *Cell* 2009; **139**: 871–890.
- Cao Y. Opinion: emerging mechanisms of tumour lymphangiogenesis and lymphatic metastasis. *Nat Rev* 2005; **5**: 735–743.

26. Magnúsdóttir E, Kalachikov S, Mizukoshi K, Savitsky D, Ishida-Yamamoto A, Panteleyev AA *et al*. Epidermal terminal differentiation depends on B lymphocyte-induced maturation protein-1. *Proc Natl Acad Sci USA* 2007; **104**: 14988–14993.
27. Li X, Deng W, Nail CD, Bailey SK, Kraus MH, Ruppert JM *et al*. Snail induction is an early response to Gli1 that determines the efficiency of epithelial transformation. *Oncogene* 2006; **25**: 609–621.
28. Olmeda D, Montes A, Moreno-Bueno G, Flores JM, Portillo F, Cano A. Snai1 and Snai2 collaborate on tumor growth and metastasis properties of mouse skin carcinoma cell lines. *Oncogene* 2008; **27**: 4690–4701.
29. Brabletz T, Jung A, Spaderna S, Hlubek F, Kirchner T. Opinion: migrating cancer stem cells - an integrated concept of malignant tumour progression. *Nat Rev* 2005; **5**: 744–749.
30. Fuchs E. Finding one's niche in the skin. *Cell Stem Cell* 2009; **4**: 499–502.
31. Mani SA, Guo W, Liao MJ, Eaton EN, Ayyanan A, Zhou AY *et al*. The epithelial-mesenchymal transition generates cells with properties of stem cells. *Cell* 2008; **133**: 704–715.
32. De Craene B, Bex G. Snail in the frame of malignant tumor recurrence. *Breast Cancer Res* 2006; **8**: 105.
33. Perez-Mancera PA, Perez-Caro M, Gonzalez-Herrero I, Flores T, Orfao A, de Herreros AG *et al*. Cancer development induced by graded expression of Snail in mice. *Hum Mol Genet* 2005; **14**: 3449–3461.
34. Aylon Y, Oren M. New plays in the p53 theater. *Curr Opin Genet Dev* 2011; **21**: 86–92.
35. Flores I, Blasco MA. A p53-dependent response limits epidermal stem cell functionality and organismal size in mice with short telomeres. *PLoS One* 2009; **4**: e4934.
36. Doody GM, Stephenson S, Tooze RM. BLIMP-1 is a target of cellular stress and downstream of the unfolded protein response. *Eur J Immunol* 2006; **36**: 1572–1582.
37. Raymond K, Richter A, Kreft M, Frijns E, Janssen H, Slijper M *et al*. Expression of the orphan protein Plet-1 during trichilemmal differentiation of anagen hair follicles. *J Invest Dermatol* 2010; **130**: 1500–1513.
38. Jensen KB, Driskell RR, Watt FM. Assaying proliferation and differentiation capacity of stem cells using disaggregated adult mouse epidermis. *Nat Protoc* 2010; **5**: 898–911.
39. Vollmers A, Wallace L, Fullard N, Hoher T, Alexander MD, Reichelt J. Two- and three-dimensional culture of keratinocyte stem and precursor cells derived from primary murine epidermal cultures. *Stem Cell Rev* 2012; **8**: 402–413.
40. Thiboutot D, Jabara S, McAllister JM, Sivarajah A, Gilliland K, Cong Z *et al*. Human skin is a steroidogenic tissue: steroidogenic enzymes and cofactors are expressed in epidermis, normal sebocytes, and an immortalized sebocyte cell line (SEB-1). *J Invest Dermatol* 2003; **120**: 905–914.
41. Desai S, Bolick SC, Maurin M, Wright KL. PU.1 regulates positive regulatory domain I-binding factor 1/Blimp-1 transcription in lymphoma cells. *J Immunol* 2009; **183**: 5778–5787.

Supplementary Information accompanies this paper on Cell Death and Differentiation website (<http://www.nature.com/cdd>)